PLOS ONE

RESEARCH ARTICLE

Croton tiglium essential oil compounds have anti-proliferative and pro-apoptotic effects in A549 lung cancer cell lines

Qing-lin Niu[1]*, Hui Sun[2]*, Chao Liu[2], Juan Li[3], Chang-xu Liang[4], Rui-rui Zhang[2], Fu-rong Ge[1], Wei Liu[1]

1 Shandong Provincial Key Laboratory of Fruit Tree Biotechnology Breeding, Shandong Institute of Pomology, Tai'an, Shandong, China, **2** Key Laboratory of Novel Food Resources Processing, Ministry of Agriculture and Rural Affairs/Key Laboratory of Agro-Products Processing Technology of Shandong Province/Institute of Agro-Food Science and Technology, Shandong Academy of Agricultural Sciences, Jinan, Shandong, China, **3** Taian Traditional Chinese Medicine Hospital, Tai'an, Shandong, China, **4** School of Water Conservancy and Environment, University of Jinan, Jinan, Shandong, China

* niuqinglin_sdau@163.com (Q-IN); sunhuiyinghua@126.com (HS)

Citation: Niu Q-l, Sun H, Liu C, Li J, Liang C-x, Zhang R-r, et al. (2020) Croton tiglium essential oil compounds have anti-proliferative and pro-apoptotic effects in A549 lung cancer cell lines. PLoS ONE 15(5): e0231437. https://doi.org/10.1371/journal.pone.0231437

Editor: Salvatore V. Pizzo, Duke University School of Medicine, UNITED STATES

Received: September 18, 2019

Accepted: March 16, 2020

Published: May 1, 2020

Data Availability Statement: All relevant data are within the paper and its Supporting Information files.

Funding: this study was supported by the Provincial Key Research and Development Program of Shandong, China (NO. 2018GNC110008) and (NO. 2019GNC106016); the Provincial Natural Science Foundation of Shandong of China (NO. ZR2016CB43);the Provincial Natural Science Foundation Key Project of Shandong, China (NO. ZR2018ZC0944).The funders had no

Abstract

As a traditional Chinese medicine, *Croton tiglium* has the characteristics of laxative, analgesic, antibacterial and swelling. This study aimed to analyze the chemical composition of *C. tiglium* essential oil (CTEO) extracted from the seeds of *C. tiglium* and its cytotoxicity and antitumor effect *in vitro*. Supercritical CO_2 fluid extraction technology was used to extract CTEO and the chemical constituents of the essential oil were identified by comparing the retention indices and mass spectra data taken from the NIST library with those calculated based on the C7-C40 *n*-alkanes standard. *In vitro* cytotoxicity of the CTEO was assessed against cancer cell lines (A549) and the human normal bronchial epithelial cells (HBE) using the CCK-8 assay. Proliferation was detected by colony formation experiments. Wound scratch and cell invasion assays were used to detect cell migration and invasion. Levels of apoptotic markers, signaling molecules, and cell cycle regulators expression were characterized by Western blot analysis. As the results, twenty-eight compounds representing 92.39% of the total oil were identified in CTEO. The CTEO has significant antitumor activity on A549 cancer cells (IC_{50} 48.38 μg/mL). *In vitro* antitumor experiments showed that CTEO treatment significantly inhibited the proliferation and migration of A549 cells, disrupted the cell cycle process, and reduced the expression levels of cyclin A, cyclin B and CDK1. CTEO can also reduce mitochondrial membrane potential, activate caspase-dependent apoptosis pathway, and finally induce apoptosis. CTEO may become an effective anti-cancer drug and will be further developed for cancer treatment.

Introduction

Lung cancer is the most common and lethal cancer worldwide, especially in developing countries [1]. It is estimated that 1,540,050 cases of lung cancer occurred in 2018 accounting for a

role in study design, data collection and analysis, decision to publish, or preparation of the manuscript. The funders had no role in study design, data collection and analysis, decision to publish, or preparation of the manuscript.

Competing interests: The authors declare that they have no conflicts of interest.

quarter of deaths in the United States [2]. Among all lung cancer patients, non-small-cell lung cancer (NSCLC) is the major type and accounted for about 80–85% [3]. NSCLC patients show high metastasis potential, and approximately 70% patients have metastases to regional lymph nodes or to distant sites upon the initial detection of cancer [4]. In addition, the vast majority of patients are diagnosed at a late stage [5]. Despite advances in treatments of NSCLC, prognosis remains a challenging aspect of this uncontrolled systemic disease.

Plant essential oils are extracted commonly from fruits, leaves, branches, and seeds of aromatic plants [6]. Due to the strong toxicological effect of the chemical synthetic products, the components of natural essential oil are gaining increasing interest and frequent presence in studies investigating their potential functional utility [7, 8]. Essential oils has anti-inflammatory, antibacterial, anti-tumor, anti-oxidation and other functions and are abundantly used in indigenous medicines, food flavoring, drug and cosmetic industries [9–11]. About 300 plant essential oils are crucial in agricultural, cosmetic, food, and health industries.

As one genus of the Euphorbiaceae family, *Croton* consists of approximately 1300 species which are widely distributed in tropical and sub-tropical regions [12]. *C. tiglium* is one of the genus *Croton* and its seeds are well known as "Badou" in mainland China and utilized widely to treat gastrointestinal disorders, intestinal inflammation, rheumatism, headache, peptic ulcer, and visceral pain [13]. In 1963, the tumor-promoting principles of *C. tiglium* seeds were reported by Van Duuren [14]. After that, many bioactive phorbol esters were isolated and evaluated from this species. The major constituent, 12-O-tetradecanoylphorbol-13-acetate (TPA), has been used widely in biochemical experiments as standard tumor-promoting agent [15, 16]. However, the chemical composition of the plant directly results in the uses and treatments of different diseases. Except phorbol esters, diverse types of diterpenes were isolated and evaluated from this species based on the previous studies investigating [17, 18], and many of them exhibited remarkable anticancer activity and inhibition vessel formation in zebrafish [19, 20].

Previous reports showed that the *C. tiglium* essential oil (CTEO) had purgative, analgesic, antimicrobial, and inflammatory properties [13, 21]. There is an abundance of oleic acid, linoleic acid, and eicosenoic acid in a methyl-esterified sample of obtained by reflux method [22]. Although many chemical constituents of *C. tiglium* have obvious anti-tumor effects, it is not clear whether the CTEO (the low polarity fraction) also has the same effects, thus, the objective of this study is to explore the chemical composition of CTEO prepared by CO_2 supercritical fluid extraction, as well as its potential anti-cancer activities and related molecular mechanisms.

Materials and methods

Plant materials

C. tiglium fruits (brown, ellipsoidal with 6 to 7 mm in diameter) were purchased in the Chinese Herbal Medicine Market in the city of Bozhou, Anhui province, China in May, 2018. Prof. Chenggang Shan who comes from the institute of agro-food science and Technology, Shandong Academy of Agriculture Sciences (IAFST, SAAS), Jinan, China identified the species. A specimen (No.18-05-05) (Fig 1A) was deposited at the Laboratory of Bioactive Substances & Functional Foods, IAFST, SAAS.

Essential oil extraction by supercritical fluid extraction

The purchased *C. tiglium* fruits (1.0 kg) are placed in the shade to dry and then ground into powder through a 40-mesh screen (450 μm), following extracted with CO_2 in a supercritical extraction vessel (25 MPa, 35˚C). The essential oil (Fig 1B) was obtained after 30 min static extraction following 30 min dynamic extraction with a flow rate of 2 L CO_2/min. The

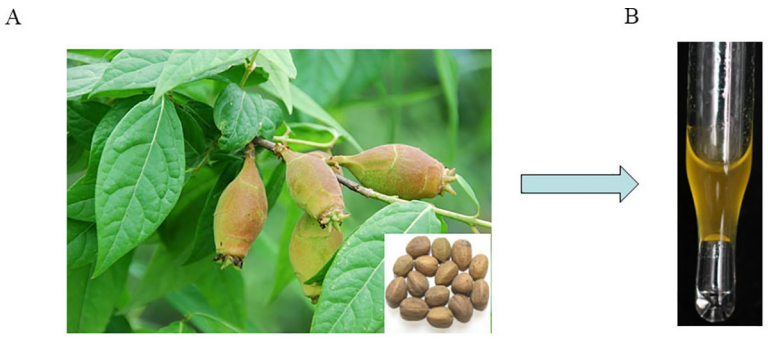

Fig 1. Morphological observation of *C. tiglium* fruits (A) and essential oil extracted by supercritical CO_2 extraction (B).

https://doi.org/10.1371/journal.pone.0231437.g001

SFE-CO_2 extracts were collected in opaque bottles, weighed, and stored in a refrigerator at 4˚C for the next experiment.

GC/MS analysis

GC-MS analysis of CTEO was performed on an Agilent 6890B GC coupled with a 5977A mass selective detector (MSD; Agilent, Santa Clara, CA, USA). An HP-5MS capillary column (30 m × 0.25 mm, 0.25 μm film thickness; Restek Corporation, Bellefonte, PA, USA) was used. Helium was used as the carrier gas at 1 mL/min with the following temperature program: initial temperature at 100˚C, increased to 200˚C at the rate of 6˚C/min, then 4˚C/min up to 300˚C and held for 10 min, for a total run of 51.7 min. The CTEO samples (1 μL) were injected at a temperature of 280˚C with a split ratio of 1/70 over 1 min. An electron impact ionization system with ionization energy of 70 eV and electron ionization spectra with a mass scan range of 30–500 *m/z* was used.

Identification of the essential oil components

Identification of the components of CTEO was conducted as described by Zhang *et al*. [22, 23], by comparing the mass spectra of the CTEO components with those from the NIST 08 mass spectra libraries and by comparing the calculated experimental GC retention indices determined using a mixture of a homologous series of normal alkanes from C7 to C40 in hexane under the same conditions described above with the GC retention indices reported in the NIST Standard Reference Database (NIST Chemistry WebBook, 2014, http://webbook.nist.gov/chemistry/). The percentage ratios of the CTEO components were computed using the normalization method of the GC/FID peak areas.

Cell culture

A549 and HBE cells were purchased from the Cell Bank of Type Culture Collection of the Chinese Academy of Sciences (Shanghai, China). A549 cells and HBE cells were cultured in RPMI-1640 (HyClone) containing 10% foetal bovine serum (Gibco) and 100 U/mL penicillin-streptomycin (HyClone). All cells were cultured at 37˚C containing 5% CO_2 humidified conditions.

CCK-8 assays

CCK-8 Kit was used to detect the cell viability. In brief, 5000 cells per wells were seeded into 96-well plates for 24 h. Following treatment with different doses of CTEO for 24, 48 and 72 h,

10 μL CCK-8 solution was added to each well, and the cells were incubated for additional 2 h at 37˚C. The absorbance at 450 nm was assessed with a microplate reader (Bio Rad, Hercules, CA, USA) in the plate. The growth inhibition curve and half-maximal inhibitory concentration value were obtained from CCK-8 viability curves using GraphPad Prism software.

Wound scratch assay

Wound scratch assay was used to assess cancer cell migration capability. For wound healing assays, cells were seeded into 6-well plates and incubated, and the cells were scratched with a 200 μL sterile pipette tip when cells reached 90% monolayer confluent. The cancer cells were subsequently treated with different concentrations of CTEO and photographed with an inverted microscope (Olympus Corp, Tokyo, Japan) at different time points to observe the distance of cell migration. Each experiment was repeated in triplicate.

Cell invasion assays

For the invasion assay, the 24-well Transwell chamber were pre-coated with 70 μL diluted matrigel (1:2 dilutions with serum-free medium) in the upper chamber and placed in a 37 incubator for coagulation. The cancer cells (1×10^5 cells/well) were resuspended in 5% FBS RPMI-1640 medium, and were treated with CTEO or alone, and seeded in the upper chamber. The lower chamber was placed in RPMI-1640 containing 20% FBS at 37˚C in 5% CO_2. After 24 h incubation, the non-invasive cells on the upper chambers were removed via gentle scraping, and those cells attached to the lower compartment were fixed with 4% paraformaldehyde and stained with crystal violet for 15–20 min at room temperature. Then, the upper chamber was washed with PBS twice. Randomly select different fields of view to take pictures under an inverted microscope (Olympus Corporation, Tokyo, Japan).

Colony formation assay

A549 cells were seeded in 6 cm cell culture dishes (1000 cells). After 7 days, the cells were treated with various concentrations of CTEO for one week. The compounds were removed and washed with PBS per wells. Then, the cells were fixed with 4% paraformaldehyde at room temperature for 20 min, stained with Giemsa and photographed with a camera.

Cell apoptosis analysis

Cell apoptosis assay was conducted using an Annexin V- FITC/PI Apoptosis detection kit (Beyotime, Nantong, China) and analyzed the apoptotic rate by flow cytometry. The cells were treated with different concentration CTEO for 48h. A certain number of cells were collected and resuspended in 195 μL Annexin V-FITC binding buffer, followed by the addition of 5 μL of annexin v-FITC and 10 μL of PI to mix. Then, the samples were incubated at room temperature for 30 min in the dark and assayed by flow cytometry (FACSCalibur, BD Biosciences).

Mitochondrial membrane potential ($\Delta\Psi$m) assay

The changes in mitochondrial membrane potential (MMP) was determined by the classical JC-1 kit (Beyotime, Nantong, China). The assay method was performed following the manufacturer's instructions. A549 cells were treated with the aforementioned method. After 48 h, cells were collected in RPMI 1640 medium and 1 mL JC-1 working solution was added; then, the samples were incubated at 37˚C for 20 min. Next, the staining cells were imaged using a confocal microscope (Nikon Corp, Tokyo, Japan).

Western blot analysis

A549 cells were treated with different concentration CTEO for 48 h. After washing with ice-cold PBS, the cells were collected and lysed using RIPA lysis buffer with a protease inhibitor (Beyotime, Nantong, China). The cell lysates were subsequently centrifuged at 12000 g at 4˚C for 15 min, and the proteins concentration were quantified by a BCA Protein Assay Kit (Beyotime, Nantong, China). About 50 μg proteins were subjected to 10% or 12% SDS-PAGE, and subsequently transferred onto PVDF membranes. The membranes were blocked with TBST containing 5% nonfat milk for 2 h at room temperature. Then, the blocked membranes were incubated overnight at 4˚C with primary antibodies: rabbit polyclonal antibody to PCNA (1:1000; GB11010-1, Servicebio Technology), Cyclin A (1:1000; 91500S, Cell Signaling Technology), Cyclin B (1:500; GB11255, Servicebio Technology), CDK1 (1:500; GB11398, Servicebio Technology), P21 (1:500; BS1269, Bioworld Technology), p-FAK (1;500; BS4617,Bioworld Technology), FAK (1:1000; 12636-1-AP, Proteintech Technology), Bax (1:1000; GB11007, Servicebio Technology), BcL-2 (1:1000; BS1511, Bioworld Technology), cleaved caspase-3 (1:1000; 9661, Cell Signaling Technology), cleaved caspase-9 (1:1000; 7237, Cell Signaling Technology), cleaved PARP (1:1000; 56255,Cell Signaling Technology). Mouse polyclonal antibody to cytochrome C (1:1000; 66264-1-Ig, Proteintech Technology), GAPDH (1:1000; GB12002, Servicebio Technology) followed by incubation with secondary antibody for HRP-conjugated Affinipure Goat Anti-Mouse IgG(H+L) (1:1000; SA00001-1, Proteintech Technology) and HRP-conjugated Affinipure Goat Anti- rabbit IgG(H+L) (1:1000; SA00001-2, Proteintech Technology) at room temperature for 2 h with rocking. Then the proteins were detected using an ECL kit in Chemiluminescence imaging system. The results were normalized to GAPDH using ImageJ software.

Statistical analysis

All experiments were repeated at least three times. The result were expressed as the mean ± standard deviation (SD) error of the mean. T test between groups were assessed by two-tailed Student. $P<0.05$ was considered to indicate a statistically significant difference.

Results

Identification of the chemical constituents of CTEO

The CTEO extracted by SFE-CO_2 was faint yellow oil (Fig 1B) with a yield of 2.51 ± 0.02% (w/w) in view of the dry weight of *C. tiglium* fruits. In order to determine volatile composition, the CTEO was analysed by GC-MS. As shown in Table 1 and S1 Fig, twenty-eight compounds were identified which is accounting for 92.39% of the total oil. The foremost compounds were 17-Octadecynoic acid at 36.73% followed by Tetradecanoic acid (8.49%), 17-Octadecynoic acid methyl ester (8.17%), *n*-Hexadecanoic acid (6.45%), *n*-Decanoic acid (5.28%), Linoleic acid ethyl ester (4.37%), and i-Propyl 9-octadecenoate (4.19%). Fatty acid and related esters, which consists of 17 compounds, are the main component of the CTEO.

CTEO inhibits the viability of A549 lung cancer cells

In order to assess the effects of CTEO on the viability of A549 lung cancer cells, after the treatment of CTEO at varied doses for 48 h, the cytotoxic activities were evaluated using a CCK-8 assay. As shown in (Fig 2A), it was observed that CTEO display significant anticancer effect with the increasing of drug concentrations. The IC_{50} of CTEO in A549 cells at 48 h was 48.38 μg/mL. The inhibition rate of the cells increases with the increase of the treatment time. When the treatment time was at 72 h, the IC_{50} value of CTEO in A549 cells was 30.7 μg/mL, as

Table 1. Chemical composition of CTEO by supercritical CO_2 fluid extraction.

Num	RT[a]	RI_{lit}[b]	RIca[c]	Compound	Formula	%
1	6.72	1191	1191	1-Dodecyne	$C_{12}H_{22}$	0.35
2	7.161	1317	1316	2,4-Decadienal	$C_{10}H_{16}O$	0.54
3	8.477	1373	1386	*n*-Decanoic acid	$C_{10}H_{20}O_2$	5.28
4	8.912	1409	1409	1a,2,3,4,4a,5,6,7b-octahydro-1,1,4,7-tetramethyl-, 1H-Cycloprop[e]azulene	$C_{15}H_{24}$	0.24
5	12.105	1475	1475	Undecanoic acid	$C_{11}H_{22}O_2$	2.54
6	12.168	1477	1477	*γ*-Himachalene	$C_{15}H_{24}$	0.21
7	15.91	1768	1782	Tetradecanoic acid	$C_{14}H_{28}O_2$	8.49
8	18.244	1926	1914	Hexadecanoic acid methyl ester	$C_{17}H_{34}O_2$	0.25
9	19.389	1968	1977	*n*-Hexadecanoic acid	$C_{16}H_{32}O_2$	6.45
10	19.492	1993	1983	Hexadecanoic acid, ethyl ester	$C_{18}H_{36}O_2$	0.66
11	21.06	2063	2067	9-Octadecen-1-ol, (Z)-	$C_{18}H_{36}O$	0.24
12	21.34	2092	2082	9,12-Octadecadienoic acid (Z,Z)-, methyl ester	$C_{19}H_{34}O_2$	0.95
13	21.466	2091	2089	9-Octadecenoic acid (Z)-, methyl ester	$C_{19}H_{36}O_2$	0.36
14	22.639	2151	2150	17-Octadecynoic acid, methyl ester	$C_{19}H_{34}O_2$	8.17
15	22.771	2162	2157	Linoleic acid ethyl ester	$C_{20}H_{36}O_2$	4.37
16	23.406	2199	2190	17-Octadecynoic acid	$C_{18}H_{32}O_2$	36.73
17	23.469	2192	2193	i-Propyl 9-octadecenoate	$C_{21}H_{40}O_2$	4.19
18	26.524	1849	1853	Z-(13,14-Epoxy)tetradec-11-en-1-ol acetate	$C_{16}H_{28}O_3$	1.20
19	27.823	2393	2422	Gibberellic acid	$C_{19}H_{22}O_6$	0.66
20	29.334	2010	2002	9-Octadecenal	$C_{18}H_{34}O$	0.64
21	31.737	2651	2633	Fumaric acid, 4-octyl dodec-2-en-1-yl ester	$C_{24}H_{42}O_4$	0.60
22	32.567	2655	2679	1-Hydroxy-3-methoxypropan-2-yl octadeca-9,12-dienoate	$C_{22}H_{40}O_4$	3.11
23	32.641	2707	2684	9,12-Octadecadienoic acid, 2-hydroxy-1-(hydroxymethyl)ethyl ester	$C_{21}H_{38}O_4$	1.56
24	36.126	2508	2484	13-Docosenoic acid, methyl ester	$C_{23}H_{44}O_2$	0.35
25	40.125	2139	2144	cis-Vaccenic acid	$C_{18}H_{34}O_2$	0.39
26	41.487	3200	3217	β-Sitosterol	$C_{29}H_{50}O$	0.91
27	42.506	3277	3282	5-Ethyl-6-methylheptan-2-yl)-3-methoxy-10,13-dimethyl-2,3,4,7,8,9,10,11,12,13,14,15,16,17-tetradecahydro-cyclopenta[a]phenanthrene	$C_{30}H_{52}O$	2.95
28	49.973	3696	3669	Oleyl oleate	$C_{36}H_{68}O_2$	0.67
Total content of identified compounds						92.39

[a]Retention time

[b]Retention index taken from NIST

[c]Retention index experimentally calculated based on the C7-C40 *n*-alkanes standard

https://doi.org/10.1371/journal.pone.0231437.t001

shown in (Fig 2B). However, the effects of CTEO on the human normal bronchial epithelial cells (HBE) were less inhibited and CTEO exhibited an IC_{50} value >100 μg/mL, as shown in (Fig 1C).

To further investigate the anti-cancer effect of CTEO, the colony formation assay was used. The number of colony formation was obviously decreased after treatment with 40 μg/mL or 60 μg/mL in A549 cells (Fig 2D). In addition, we detected the expression of proliferation cell nuclear antigen (PCNA) as a biomarker of proliferation. As shown in Fig 2E, the expression of PCNA was reduced in A549 cells after CTEO treatment, which was consistent with that of the CCK-8 assay and colony formation assay. Thus, CTEO appears to inhibit the proliferation of A549 cells.

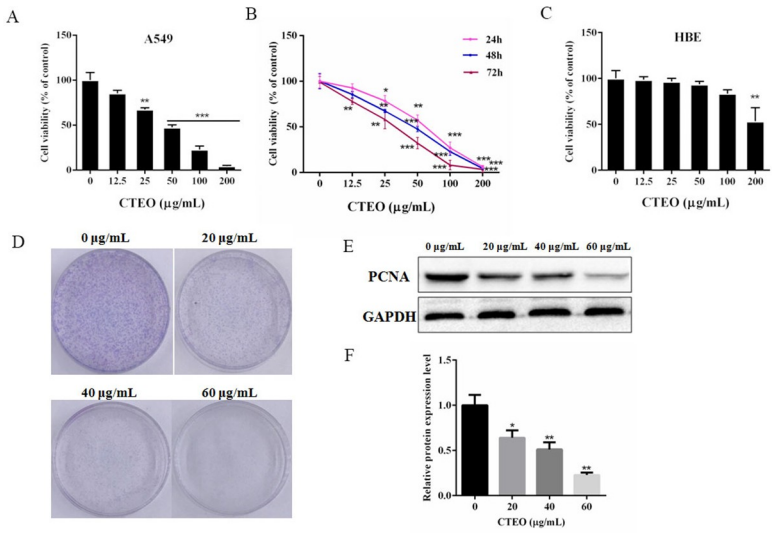

Fig 2. CTEO inhibits the viability of A549 lung cancer cells. A.The viability of A549 cells following 48 h of CTEO treatment was detected by CCK-8 assay. B. A549 cells were cultured with different concentrations (0–200 μg/mL) of CTEO for varied time points). Cell viability was determined by CCK-8 assay. C. The viability of HBE cells following 48 h of CTEO treatment was detected by CCK-8 assay. D. The colony formation of A549 cells was determined with colony formation assay after exposure to different concentrations of CTEO (0, 20, 40 and 60 μg/mL) and colonies were allowed to grow for 10 days. E, F. Western blotting analysis of PCNA protein expression after CTEO treatment, and quantification. Values represent mean ± SD of three independent experiments. $^{*}P < 0.05$, $^{**}P < 0.01$, and $^{***}P < 0.001$.

https://doi.org/10.1371/journal.pone.0231437.g002

CTEO suppressed cell-cycle progression in A549 cancer cells

To study the cellular mechanisms of how CTEO inhibits cell proliferations, we analyzed the changes in the expression levels of cell cycle factors related proteins in A549 cells. We assumed that CTEO treatment may impair the cyclin related proteins expressions in A549 cells. To verify this hypothesis, we detected the protein levels of cyclin proteins, such as cyclin A, cyclin B,

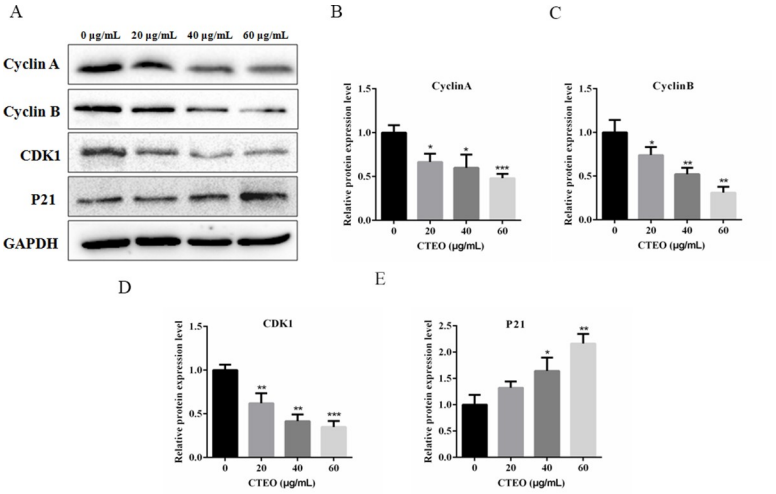

Fig 3. CTEO suppressed cell-cycle progression in A549 cells. A-E, The expression of cell cycle related protein cyclin A, cyclin B, CDK1 and P21 in A549 cells following 48 h of different concentrations CTEO treatment were detected by western blot analysis, and quantification. Values represent mean ± SD of three independent experiments. $^{*}P < 0.05$, $^{**}P < 0.01$, and $^{***}P < 0.001$.

https://doi.org/10.1371/journal.pone.0231437.g003

CDK1 and P21 after treatment of different concentrations of CTEO for 48 h. The biochemical results showed that the expression levels of cyclin A, cyclin B and CDK1 were all reduced dramatically by CTEO treatment. However, P21, cyclin dependent kinase inhibitor, its expression significantly increased in a concentration-dependent manner after treated with CTEO (Fig 3A–3E). Taken together, all the results indicate that CTEO may decrease cyclin protein expressions at least partly, finally resulting in cell cycle arrest and cell growth inhibition.

CTEO inhibits the migratory and invasive ability of A549 cells

To detect the effect of CTEO on migratory and invasive capabilities of A549 cells, wound scratch assay and transwell invasion assay were performed on A549 cells. It noted that, for A549 cells treated with 40 μg/mL CTEO, their wound healing rate was markedly decreased when compared with 0 μg/mL CTEO on the basis of these results. We also noted that, compared with A549 cells treated with 0 μg/mL CTEO, those treated with 40 μg/mL CTEO had dramatically lower invasive cell numbers, as shown in (Fig 4).

CTEO inhibited the activation of FAK in A549 Cells

FAK plays a significant part in many types of cell events, such as proliferation, survival, apoptosis, migration and invasion. The above experiments have demonstrated that CTEO could significantly inhibit A549 cell migration and invasion. However, it still needs to continue to further verify whether CTEO can inhibit the metastasis and invasion of A549 cells through the FAK pathway. In the present study, A549 cells were treated with CTEO (0, 20, 40, 60 μg/mL) for 48 h. As shown in (Fig 5), the group which was treated with CTEO significantly decreased p-FAK level, but has no effect on the expression of FAK. These results suggested that reduced the expression of p-FAK may increase its inhibitory activity of cell migration and invasion.

CTEO promoted A549 cells apoptosis in a dose-dependent manner

To determine whether CTEO could induce A549 cell apoptosis, the A549 cells were treated with varying concentrations of CTEO for 48 h and cells for changes in apoptotic markers was analyzed by flow cytometer. As shown in Fig 6A, the results of Annexin-V-FITC/PI exhibited that the apoptosis rate was significantly increased after the cells were treated with 20 μg/mL CTEO by the contrast of the 0 μg/mL group. And as the concentration increases, the number of cell apoptosis increases in a concentration-dependent manner (32.6% at 40 μg/mL, 42.5% at 60 μg/mL).

Subsequently, in order to study the mechanism that mediates CTEO-induced apoptosis, the expression of Bcl-2 and Bax in CTEO treatment of A549 cells was determined using a Western blot assay. The results demonstrated that the significant increase in the ratio of Bax/Bcl2 protein, the expression of the anti-apoptotic protein Bcl-2 was decreased, while the expression of the pro-apoptotic proteins Bax were increased in CTEO group compared with the corresponding values in control group. As shown in (Fig 6C); $P<0.05$. The results indicated that CTEO may promote the apoptosis of A549 cells.

CTEO induces mitochondrial dysfunction in A549 cells

As we all know, the mitochondria play an important part in the regulation of cell apoptosis. Mitochondrial membrane potential collapse is an early feature of cell apoptosis. JC-1 staining was used to assess the loss of mitochondrial membrane potential by fluorescence microscope and western blotting to evaluate related protein expression in A549 cells. As shown in Fig 7A, the results certified that with the increase of CTEO (0, 20, 40 and 60 μg/mL), the green

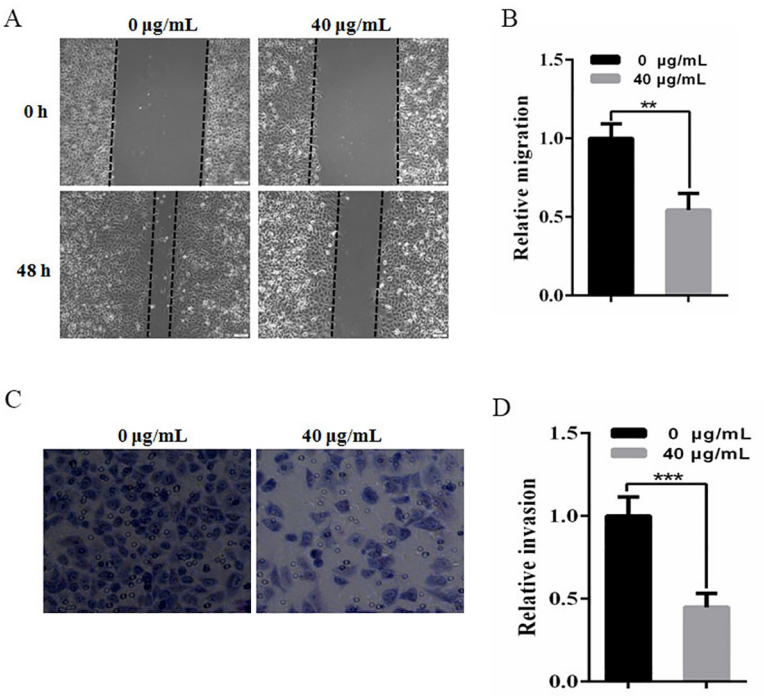

Fig 4. CTEO inhibits the migratory and invasive ability of A549 cells. A,B. Wound healing assay. A549 cells were treated with CTEO and artificial scratches were done with sterile 200 μL pipette. Photographs were taken after treatment. C,D. Transwell invasion chamber assay. The cells were treated the concentration indicated by CTEOfor 48 h. Cells invading the basement membrane were stained with Giemsa. Values represent mean ± SD of three independent experiments. $^{*}P < 0.05$, $^{**}P < 0.01$, $^{***}P < 0.001$ compared with the untreated control (dose 0).

https://doi.org/10.1371/journal.pone.0231437.g004

fluorescence gradually increased while the red fluorescence gradually decreased, indicating that the mitochondrial membrane potential gradually decreased. Subsequently, we also examined the changes of cytochrome C in A549 cells. The results demonstrated that the protein expression level of Cytochrome C in the cytoplasm gradually increased with the increase of CTEO concentration, as shown in Fig 7B.

CTEO induces apoptosis via caspase-mediated pathways in A549 cells

Cysteine proteases can transmit apoptotic signals in the proteolytic cascade, after caspase cleaving, it can activate other caspase enzymes and subsequently degrades cellular targets that cause cell death. The above results indicated that CTEO treatment led to reduce in the ratio of Bcl2/ Bax protein, and an increase in the expression level of Cytochrome C in the cytoplasm.

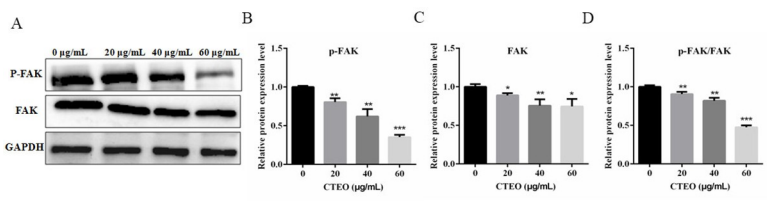

Fig 5. CTEO inhibited the activation of FAK in A549 cells. A-C. The expression of FAK and p-FAK protein in A549 cells following 48 h of different concentrations CTEO treatment were detected by western blot analysis, and quantification. C. The ratio of FAK to p-FAK protein expression was quantified analysis. Values represent mean ± SD of three independent experiments. $^{*}P < 0.05$, $^{**}P < 0.01$, and $^{***}P < 0.001$.

https://doi.org/10.1371/journal.pone.0231437.g005

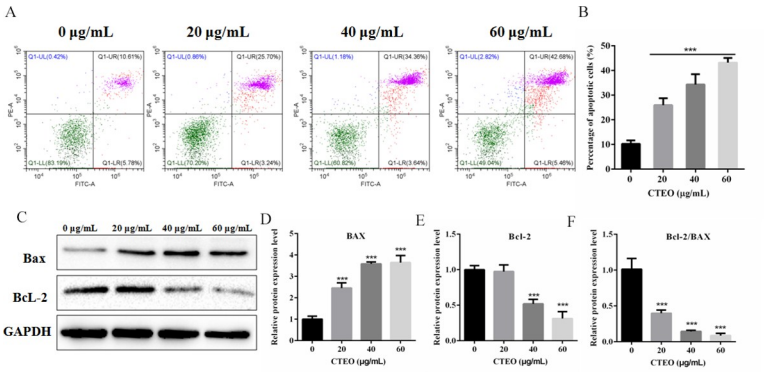

Fig 6. CTEO promoted A549 cells apoptosis in a dose-dependent manner. A, B. The apoptosis of A549 cells following 48 h of different concentrations CTEO treatment was detected by flow cytometry, and quantification. C-F. The expression of Bax and Bcl-2 protein in A549 cells following 48 h of different concentrations CTEO treatment were detected by western blot analysis, and quantification. Values represent mean ± SD of three independent experiments. $^{*}P < 0.05$, $^{**}P < 0.01$, and $^{***}P < 0.001$.

https://doi.org/10.1371/journal.pone.0231437.g006

To investigate the potential mechanism of cell apoptosis and whether CTEO induce apoptosis in A549 cells via a caspase-mediated pathway. We assessed the apoptotic markers in A549 cells by gradient CTEO treatment using Western blot analysis. As shown in Fig 8A, the level of cleaved caspase-3, cleaved caspase-9 were markedly up-regulated by CTEO in the A549 cells, and the level of cleaved PARP was also significantly increased compared with the control.

Discussions

Lung cancer is one of the most common malignancies in the world, and its high incidence and recurrence rate are the leading causes of cancer death [24]. Uncontrolled mitosis and rapid migration and migration of cancer cells are hallmarks of cancer, which are associated with poor prognosis in many tumors, such as lung, breast and osteosarcoma [25, 26]. Thus, targeting inhibition of cell proliferation or promoting apoptosis can provide clues to cancer

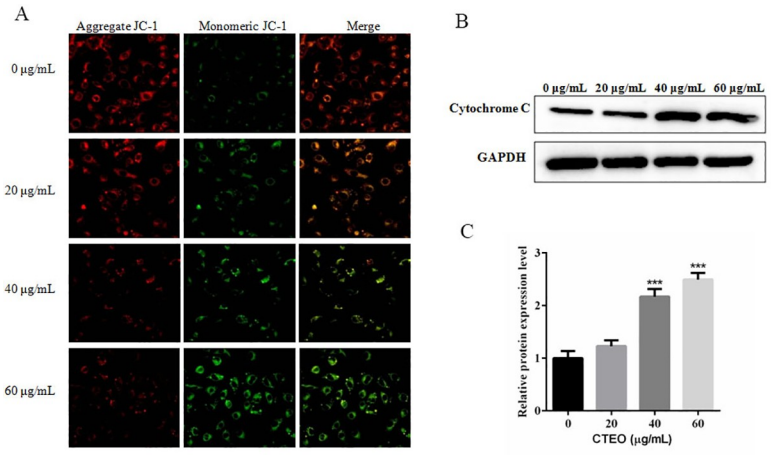

Fig 7. CTEO induces mitochondrial dysfunction in A549 cells. A. The change of mitochondrial membrane potential in A549 cells following 48 h of different concentrations CTEO treatment was detected by JC-1 staining analysis. B, C. The expression of cytochrome C protein in A549 cells following 48 h of different concentrations CTEO treatment were detected by western blot analysis, and quantification. Values represent mean ± SD of three independent experiments. $^{*}P < 0.05$, $^{**}P < 0.01$, and $^{***}P < 0.001$.

https://doi.org/10.1371/journal.pone.0231437.g007

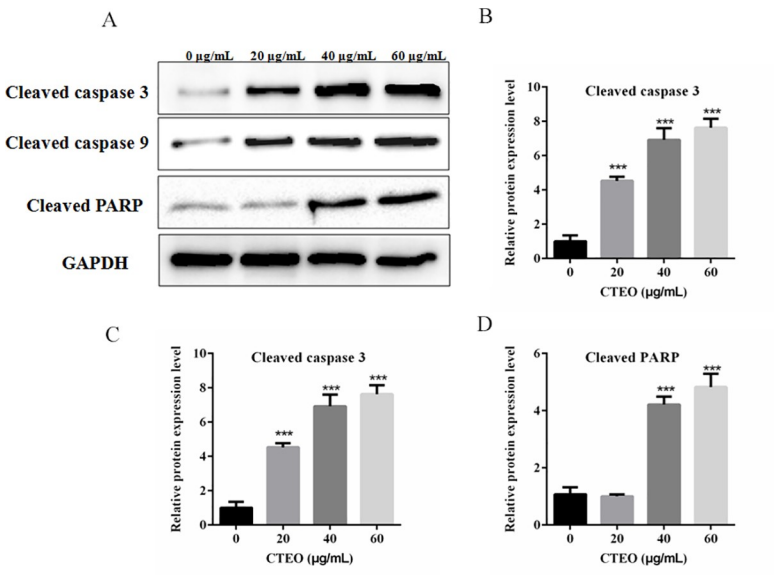

Fig 8. CTEO induces apoptosis via caspase-mediated pathways in A549 cells. A-D. The expression of apoptosis-related protein in A549 cells following 48 h of different concentrations CTEO treatment were detected by western blot analysis, and quantification. Values represent mean ± SD of three independent experiments. $^{*}P < 0.05$, $^{**}P < 0.01$, and $^{***}P < 0.001$.

https://doi.org/10.1371/journal.pone.0231437.g008

treatment. Previous reports showed that there are abundant of linoleic acid, oleic acid and eicosenoic acid in the seeds oil extracted with petroleum from Chinese *C. tiglium*. Instead, carcinogenic and anti-HIV-1 active ingredient may be very rare in the sample, and it is difficult to obtain by conventional extraction and separation method [27]. Therefore, in this study, the essential oil of *C. tiglium* was obtained by alternative technique (SFE) firstly for the further research.

One study has previously reported on the chemical composition of CTEO, and from which 17 fat acid components were identified. The main components were linoleic acid, oleic acid, and eicosenoic acid in ethy-esterified sample, occupying 77.33% of the total oil. In our present study, the mainly chemotypes of identified compounds are also fatty acid, these results are consistent with that previously reported [28]. However, many volatile compounds that had not been reported in previous studies were identified, such as 17-Octadecynoic acid (36.73%), Tetradecanoic acid (8.49%), *n*-Hexadecanoic acid (6.45%), Undecanoic acid (2.54%) etc.. In addition, this alternative technique (SFE) generates very more chemical components (28 compounds were identified) than those obtained by petroleum extraction, which will benefit for further processing of the *C. tiglium* plants.

As described in a previous paper [29]. To study the cytotoxicity of essential oils, an IC_{50} value which less than 50 μg/mL represents a strong cytotoxic activity. In addition, IC_{50} values between 50–100, 100–200 and 200–300 μg/mL represent moderate, weak and very weak cytotoxicity, respectively. With this in mind, the IC_{50} value of CTEO in this study was 48.38 μg/mL, indicating strong cytotoxicity against A549 cells (Fig 2). Therefore, the essential oil obtained from *C. tiglium* has great potential as a source of natural anti-cancer drugs.

In the present study, CTEO showed significant antitumor activity attributable to the presence of fatty acids, which accounted for 78.48% of the total oil (Table 1). Previous studies have demonstrated that fatty acids have significant anti-tumor effects [30]. Butyrate, histone deacetylase inhibitor, is a typical short chain fatty acid, which have significant anti-cancer activity against colon cancer cell line HCT116. Correlation analysis showed that butyrate treatment

significantly inhibited the proliferation of HCT116 cells and increased the ratio of Bax/Bcl-2 protein to induce apoptosis [31]. Nitro-Fatty Fatty Acid (NFA) is an endogenous lipid mediator. It has been found that NFA exerts a strong anti-cancer effect on colorectal cancer (CRC) cells and inhibits the viability of CRC cells (HCT-116 and HT-29). The mitochondrial endogenous apoptotic pathway induces caspase-dependent apoptosis. Therefore, the total oil is selected to study the relevant mechanisms of the observed effects.

PCNA, as a biomarker of proliferation, the expression was down-regulated in A549 cells after CTEO treatments (Fig 2). The inhibitory effect of CTEO was further confirmed by colony formation assay. These results indicate that CTEO has an inhibitory effect on A549 cell growth *in vitro*. Cell proliferation is dependent on the progression of the cell cycle. Another very important mechanism used by anticancer agents is cell cycle arrest. If the cancer cell were arrested in any phase of the cell cycle, they are unable to complete cell division and tumor growth is inhibited [30]. Moreover, the proliferative inhibitory effects of CTEO on A549 cells may be at least partly dependent on cyclin protein expressions, because it was noted that CTEO treatment would inhibit cyclin protein expression (Fig 3). Thus, the reduced cyclin protein expressions may be responsive to the cell cycle arrest and consequently apoptosis.

Cancer cell metastasis is associated with various steps, including adhesion of cancer cells to ECM, degradation of the basement membrane to allow tumor cells to migrate and invade peripheral tissues [32, 33]. Many types of cell adhesion molecules play important roles in different steps of metastatic events [34]. Focal adhesion kinase (FAK) is a major mediator of signal transduction through cells and extracellular matrices and plays an important role in cell proliferation, survival, apoptosis, migration and invasion [35, 36]. FAK is phosphorylated when activated. Tyr 397 (Y397) is the main phosphorylated site. By binding with other kinase domains, FAK activates downstream signaling pathways, regulates cell migration and induces apoptosis [33]. The elevated FAK and phospho-FAK Tyr397 are associated with the development, invasion and metastasis of several tumors [37]. Previous studies [38] have shown that treatment of tumor cells with FAK-specific inhibitors could inhibit tumor cell proliferation, migration and invasion. However, in our results, CTEO was able to significantly inhibit the migration and invasion (Fig 4), and decrease p-FAK protein levels in a dose-dependent manner in A549 cells (Fig 5).

Apoptosis inhibits cancer cell survival and has been identified as a central mechanism for the induction of cell death by cytostatic drugs. Cytostatic drugs can cause apoptosis through a variety of pathways, including activation of death receptor/ligand expression, changes in mitochondrial membrane potential, ROS production, DNA damage etc [39]. Most anti-cancer drugs could promote tumor cell apoptosis by up-regulating the ratio of Bax/Bcl-2 [40]. Consistent with previous studies, our results find that CTEO could increase the protein expression of Bax and reduce the levels of Bcl-2 in A549 cells in a dose-dependent manner (Fig 6). The increased Bax/Bcl-2 ratio could cause a decrease in the mitochondrial membrane potential, resulting in the release of cytochrome c into the cytosol. Decreased mitochondrial membrane potential is an early phenomenon of tumor cell apoptosis. The released cytochrome c activates Caspase-9, and activated caspase-9 further activates caspase-3. Thus the caspase cascade is activated and PARP is cleaved to cause apoptosis [41]. Our findings revealed that CTEO caused a dramatic loss of mitochondrial membrane potential and accumulation of cleaved caspase-3 cleaved caspase-9 and cleaved PARP (Figs 7 and 8). The above results indicate that CTEO-induced caspase cascade activation together with subsequent PARP cleavage implying CTEO-mediated apoptosis occurs via the intrinsic pathway.

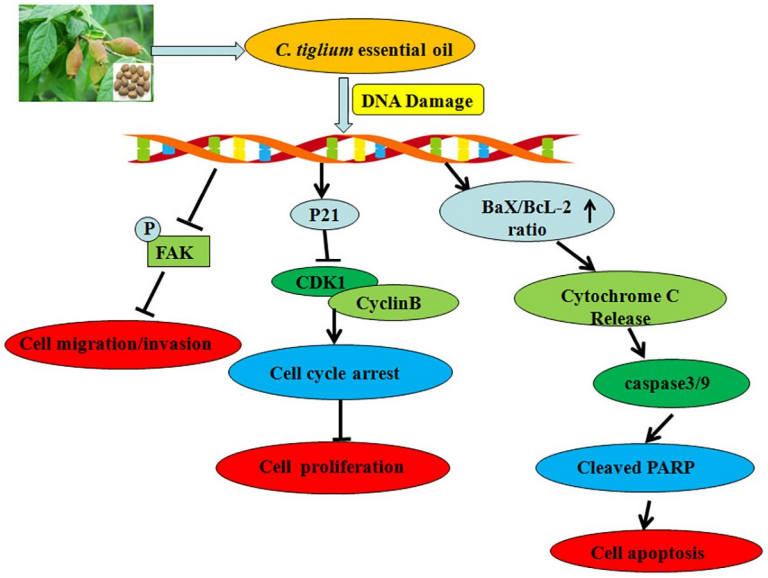

Fig 9. Proposed mechanisms of the antitumor effects of CTEO on lung cancer cells. CTEO depresses cell growth, invasion, migration and induces cell apoptosis in A549cells via (1) decreasing expression of Proliferation factors;(2) inhibiting invasion and migration factors; and (3) enhancing expression of pro-apoptotic factors.

https://doi.org/10.1371/journal.pone.0231437.g009

Conclusion

Taking these results into consideration, we propose that the anti-cancer effect of CTEO on A549 cells is partly through decreasing expression of proliferation factors, inhibiting invasion and migration factors, and enhancing expression of pro-apoptotic factors, as shown in Fig 9. Natural resources capable of inducing tumor cell cycle arrest and apoptosis are expected to be candidates for anticancer drugs [42]. Therefore, these evidences suggested that CTEO may be a promising and future supplement in the investigation of novel chemopreventive or chemotherapeutic agents for human lung cancers and may be considered for further clinical studies in drug development. These findings should benefit the development of *C. tiglium* industry.

Supporting information

S1 Fig. Composition of CTEO on HP-5MS column.
(TIF)

S2 Fig. Composition of C7-C40 alkanes on HP-5MS column.
(TIF)

S1 Raw Images. All replicates PCNA and GAPDH blots. S1-raw-images represents western blot analysis shown in Fig 2. Lanes 1–4 represent 0. 20. 40. 60 μg/mL group.
(TIF)

S2 Raw Images. All replicates cyclin A. cyclin B. CDK1. P21 and GAPDH blots. S2-raw-images represents western blot analysis shown in Fig 3. Lanes 1–4 represent 0. 20. 40. 60 μg/mL group.
(TIF)

S3 Raw Images. All replicates FAK. P-FAK and GAPDH blots. S3-raw-images represents western blot analysis shown in Fig 5. Lanes 1–4 represent 0. 20. 40. 60 μg/mL group.
(TIF)

S4 Raw Images. All replicates BAX. Bcl-2 and GAPDH blots. S4-raw-images represents western blot analysis shown in Fig 6. Lanes 1–4 represent 0. 20. 40. 60 μg/mL group.
(TIF)

S5 Raw Images. All replicates Cytochrome C and GAPDH blots. S5-raw-images represents western blot analysis shown in Fig 7. Lanes 1–4 represent 0. 20. 40. 60 μg/mL group.
(TIF)

S6 Raw Images. All replicates cleaved caspase 3. Cleaved caspase 9. Cleaved PARP and GAPDH blots. S6-raw-images represents western blot analysis shown in Fig 8. Lanes 1–4 represent 0. 20. 40. 60 μg/mL group.
(TIF)

Acknowledgments

The authors would like to thank Prof. Cheng-gang Shan for identifying the species of *C. tiglium*.

Author Contributions

Data curation: Hui Sun.

Formal analysis: Hui Sun, Juan Li.

Funding acquisition: Chao Liu.

Investigation: Hui Sun, Chao Liu, Juan Li, Fu-rong Ge, Wei Liu.

Methodology: Hui Sun, Chao Liu, Chang-xu Liang, Rui-rui Zhang.

Resources: Qing-lin Niu, Wei Liu.

Software: Qing-lin Niu.

Supervision: Chao Liu.

Validation: Qing-lin Niu, Hui Sun.

Writing – original draft: Qing-lin Niu, Rui-rui Zhang.

Writing – review & editing: Hui Sun.

References

1. Sorber L, Zwaenepoel K, Deschoolmeester V, Van Schil PE, Van Meerbeeck J, Lardon F, et al. Circulating cell-free nucleic acids and platelets as a liquid biopsy in the provision of personalized therapy for lung cancer patients. Lung Cancer. 2017; 107:100–7. Epub 2016/05/18. https://doi.org/10.1016/j.lungcan.2016.04.026 PMID: 27180141.
2. Siegel RL, KD M, A J. Cancer statistics, 2018. CA-Cancer J Clin. 2018; 68(1):7. https://doi.org/10.3322/caac.21442 PMID: 29313949
3. Scrima M, Zito MF, Oliveira DM, Marinaro C, La ME, Rocco G, et al. Aberrant Signaling through the HER2-ERK1/2 Pathway is Predictive of Reduced Disease-Free and Overall Survival in Early Stage Non-Small Cell Lung Cancer (NSCLC) Patients. J Cancer. 2017; 8(2):227–39. https://doi.org/10.7150/jca.17093 PMID: 28243327
4. Corbin KS, Hellman S, Weichselbaum RR. Extracranial oligometastases: a subset of metastases curable with stereotactic radiotherapy. J Clin Oncol. 2013; 31(11):1384–90. Epub 2013/03/06. https://doi.org/10.1200/JCO.2012.45.9651 PMID: 23460715.
5. Lv X, Cui Z, Li H, Li J, Yang Z, Bi Y, et al. Polymorphism in lncRNA AC008392.1 and its interaction with smoking on the risk of lung cancer in a Chinese population. Cancer manag Res. 2018; 10:1377–87.

Epub 2018/06/09. https://doi.org/10.2147/CMAR.S160818 PMID: 29881308; PubMed Central PMCID: PMC5985799.

6. Harkat-Madouri L, Asma B, Madani K, Said BOS, Rigou P, Grenier D, et al. Chemical composition, antibacterial and antioxidant activities of essential oil of Eucalyptus globulus from Algeria. Ind Crop Prod. 2015; 78:148–53.
7. Babahmad RA, Aghraz A, Boutafda A, Papazoglou EG, Tarantilis PA, Kanakis C, et al. Chemical composition of essential oil of Jatropha curcas L. leaves and its antioxidant and antimicrobial activities. Ind Crop Prod. 2018; 121:405–10. https://doi.org/10.1016/j.indcrop.2018.05.030 ISI:000437996900046.
8. Rakmai J, Cheirsilp B, Mejuto JC, Simal-Gandara J, Torrado-Agrasar A. Antioxidant and antimicrobial properties of encapsulated guava leaf oil in hydroxypropyl-beta-cyclodextrin. Ind Crop Prod. 2018; 111:219–25. https://doi.org/10.1016/j.indcrop.2017.10.027 ISI:000419407600028.
9. Gendy ANE, Leonardi M, Mugnaini L, Bertelloni F, Ebani VV, Nardoni S, et al. Chemical composition and antimicrobial activity of essential oil of wild and cultivated Origanum syriacum plants grown in Sinai, Egypt. Ind Crop Prod. 2015; 67:201–7.
10. Tian J, Ban X, Zeng H, He J, Huang B, Wang Y. Chemical composition and antifungal activity of essential oil from Cicuta virosa L. var. latisecta Celak. Int J Food Microbiol. 2011; 145(2):464–70.
11. Lee SY, Kim KBWR, Lim SI, Ahn DH. Antibacterial mechanism of Myagropsis myagroides extract on Listeria monocytogenes. Food Control. 2014; 42(42):23–8.
12. Salatino A, Salatino MLF, Negri G. Traditional uses, chemistry and pharmacology of Croton species (Euphorbiaceae). J Brazil Chem Soc. 2007; 18(1):11–33. https://doi.org/10.1590/S0103-50532007000100002 ISI:000245195900001.
13. Qiu HX. Flora Republicae Popularis Sinicae: Science Press: Beijing; 1996. 130 p.
14. Vanduuren BL, Orris L, Arroyo E. Tumour-enhancing Activity of the Active Principles of Croton tiglium L. Nature. 1964; 200(4911):1115–6.
15. Colburn NH, Gindhart TD, Hegamyer GA, Blumberg PM, Delclos KB, Magun BE, et al. Phorbol diester and epidermal growth factor receptors in 12-O-tetradecanoylphorbol-13-acetate-resistant and -sensitive mouse epidermal cells. Cancer Res. 1982; 42(8):3093–7. PMID: 6284358.
16. Hecker E. Cocarcinogenesis and tumor promoters of the diterpene Ester type as possible carcinogenic risk factors. J Cancer Res Clin. 1981; 99(1–2):103–24.
17. Marshall GT, Klocke JA, Lin LJ, Douglas Kinghorn A. Effects of diterpene esters of tigliane, daphnane, ingenane, and lathyrane types on pink bollworm,Pectinophora gossypiella saunders (Lepidoptera: Gelechiidae). J Chem Ecol. 1985; 11(2):191–206. https://doi.org/10.1007/BF00988202 PMID: 24309846
18. Bauer R, Tittel G, Wagner H. Isolation and detection of phorbolesters in crotonoil with HPLC. Planta med. 1983; 48(1):10. https://doi.org/10.1055/s-2007-969869 PMID: 17404933
19. Kim JH, Lee SJ, Han YB, Moon JJ, Kim JB. Isolation of isoguanosine from Croton tiglium and its antitumor activity. Archives of Pharm Res. 1994; 17(2):115–8.
20. Liebich HM, Lehmann R, Stefano C, Di, H?Ring HU, Kim JH, Kim KR. Analysis of traditional Chinese anticancer drugs by capillary electrophoresis. J Chromatography A. 1998; 795(2):388–93.
21. Tsai JC, Tsai S, Chang WC. Effect of ethanol extracts of three Chinese medicinal plants with laxative properties on ion transport of the rat intestinal epithelia. Biol Pharm Bull. 2004; 94(2):162–5.
22. Mei L, Ping W, Wang ZY, Huang XL. GC-MS Analysis of Chemical Components in Seeds Oil from Croton tiglium. J Chin Med Mater. 2012; 35(7):1105.
23. Zhang J, Huang RZ, Cao HJ, Cheng AW, Jiang CS, Liao ZX, et al. Chemical composition, in vitro antitumor activities and related mechanisms of the essential oil from the roots of Potentilla discolor. Ind Crop Prod. 2018; 113:19–27. https://doi.org/10.1016/j.indcrop.2017.12.071 ISI:000426411800003.
24. Hoffman RM, Sanchez R. Lung Cancer Screening. Med Clin North Am. 2017; 101(4):769–85. Epub 2017/06/05. https://doi.org/10.1016/j.mcna.2017.03.008 PMID: 28577626.
25. Hanahan D, Weinberg RA. Hallmarks of cancer: the next generation. Cell. 2011; 144(5):646–74. Epub 2011/03/08. https://doi.org/10.1016/j.cell.2011.02.013 PMID: 21376230.
26. Hainaut P, Plymoth A. Targeting the hallmarks of cancer: towards a rational approach to next-generation cancer therapy. Curr opin oncology. 2013; 25(1):50–1. Epub 2012/11/15. https://doi.org/10.1097/CCO.0b013e32835b651e PMID: 23150341.
27. Lan M, Wan P, Wang ZY, Huang XL. GC-MS analysis of chemical components in seeds oil from Croton tiglium. Zhong yao cai 2012; 35(7):1105–8. Epub 2012/12/21. PMID: 23252276.
28. Yang XH, Deng SM, Liang ZY, Lin Q. Composition analysis of Croton crassifolius essential oil. J Hainan University (Natural Science Edition). 2007; 25(3):262–4.

29. Sylvestre M, Pichette A, Longtin A, Nagau F, Legault J. Essential oil analysis and anticancer activity of leaf essential oil of Croton flavens L. from Guadeloupe. J Ethnopharmacol. 2006; 103(1):99–102. Epub 2005/09/20. https://doi.org/10.1016/j.jep.2005.07.011 PMID: 16168586.

30. Kuhn B, Brat C, Fettel J, Hellmuth N, Maucher IV, Bulut U, et al. Anti-inflammatory nitro-fatty acids suppress tumor growth by triggering mitochondrial dysfunction and activation of the intrinsic apoptotic pathway in colorectal cancer cells. Biochem pharm. 2018; 155:48–60. Epub 2018/06/18. https://doi.org/10.1016/j.bcp.2018.06.014 PMID: 29909078.

31. Cao M, Zhang Z, Han S, Lu X. Butyrate inhibits the proliferation and induces the apoptosis of colorectal cancer HCT116 cells via the deactivation of mTOR/S6K1 signaling mediated partly by SIRT1 downregulation. Mol med rep. 2019; 19(5):3941–7. Epub 2019/03/14. https://doi.org/10.3892/mmr.2019.10002 PMID: 30864709.

32. Mego M, Mani SA, Cristofanilli M. Molecular mechanisms of metastasis in breast cancer—clinical applications. Nat rev Clin oncol. 2010; 7(12):693–701. Epub 2010/10/20. https://doi.org/10.1038/nrclinonc.2010.171 PMID: 20956980.

33. Schultze A, Decker S, Otten J, Horst AK, Vohwinkel G, Schuch G, et al. TAE226-mediated inhibition of focal adhesion kinase interferes with tumor angiogenesis and vasculogenesis. Invest new drugs. 2010; 28(6):825–33. Epub 2009/09/29. https://doi.org/10.1007/s10637-009-9326-5 PMID: 19784551.

34. Murata J, Saiki I. Tumor metastasis and cell adhesion molecules. Gan to kagaku ryoho. 1999; 26 (5):715–23. Epub 1999/05/11. PMID: 10234306.

35. Siesser PM, Hanks SK. The signaling and biological implications of FAK overexpression in cancer. Clin Cancer Res. 2006; 12(11 Pt 1):3233–7. Epub 2006/06/03. https://doi.org/10.1158/1078-0432.CCR-06-0456 PMID: 16740741.

36. McLean GW, Carragher NO, Avizienyte E, Evans J, Brunton VG, Frame MC. The role of focal-adhesion kinase in cancer—a new therapeutic opportunity. Nat Rev Cancer. 2005; 5(7):505–15. Epub 2005/08/03. https://doi.org/10.1038/nrc1647 PMID: 16069815.

37. Weiner TM, Liu ET, Craven RJ, Cance WG. Expression of focal adhesion kinase gene and invasive cancer. Lancet. 1993; 342(8878):1024–5. Epub 1993/10/23. https://doi.org/10.1016/0140-6736(93)92881-s PMID: 8105266.

38. Lee S, Qiao JB, Paul P, O'Connor KL, Evers BM, Chung DH. Fak Is a Critical Regulator of Neuroblastoma Liver Metastasis. Oncotarget. 2012; 3(12):1576–87. ISI:000315801200018. https://doi.org/10.18632/oncotarget.732 PMID: 23211542

39. Lu DF, Wang YS, Li C, Wei GJ, Chen R, Dong DM, et al. Actinomycin D inhibits cell proliferations and promotes apoptosis in osteosarcoma cells. Int J Clin Exp Med. 2015; 8(2):1904–11. Epub 2015/05/02. PMID: 25932119; PubMed Central PMCID: PMC4402766.

40. Prabhu KS, Siveen KS, Kuttikrishnan S, Iskandarani AN, Khan AQ, Merhi M, et al. Greensporone C, a Freshwater Fungal Secondary Metabolite Induces Mitochondrial-Mediated Apoptotic Cell Death in Leukemic Cell Lines. Front pharm. 2018; 9:720. Epub 2018/08/01. https://doi.org/10.3389/fphar.2018.00720 PMID: 30061828; PubMed Central PMCID: PMC6054921.

41. Jin Z, El-Deiry WS. Overview of cell death signaling pathways. Cancer Biol Ther. 2005; 4(2):139–63. Epub 2005/02/24. https://doi.org/10.4161/cbt.4.2.1508 PMID: 15725726.

42. Wang Y, Bao XW, Zhao A, Zhang J, Zhang MY. Raddeanin A inhibits growth and induces apoptosis in human colorectal cancer through downregulating the Wnt/β-catenin and NF-κB signaling pathway. Life Sci. 2018; 207:532–49. https://doi.org/10.1016/j.lfs.2018.06.035 PMID: 29972765